



UNIVERSITY OF LEEDS

This is a repository copy of *Fungal decomposition of river organic matter accelerated by decreasing glacier cover*.

White Rose Research Online URL for this paper:
<https://eprints.whiterose.ac.uk/172046/>

Version: Supplemental Material

Article:

Fell, SC, Carrivick, JL orcid.org/0000-0002-9286-5348, Cauvy-Fraunié, S et al. (7 more authors) (2021) Fungal decomposition of river organic matter accelerated by decreasing glacier cover. *Nature Climate Change*, 11. pp. 349-353. ISSN 1758-678X

<https://doi.org/10.1038/s41558-021-01004-x>

© The Author(s), under exclusive licence to Springer Nature Limited 2021. This is an author produced version of an article, published in *Nature Climate Change*. Uploaded in accordance with the publisher's self-archiving policy.

Reuse

Items deposited in White Rose Research Online are protected by copyright, with all rights reserved unless indicated otherwise. They may be downloaded and/or printed for private study, or other acts as permitted by national copyright laws. The publisher or other rights holders may allow further reproduction and re-use of the full text version. This is indicated by the licence information on the White Rose Research Online record for the item.

Takedown

If you consider content in White Rose Research Online to be in breach of UK law, please notify us by emailing eprints@whiterose.ac.uk including the URL of the record and the reason for the withdrawal request.



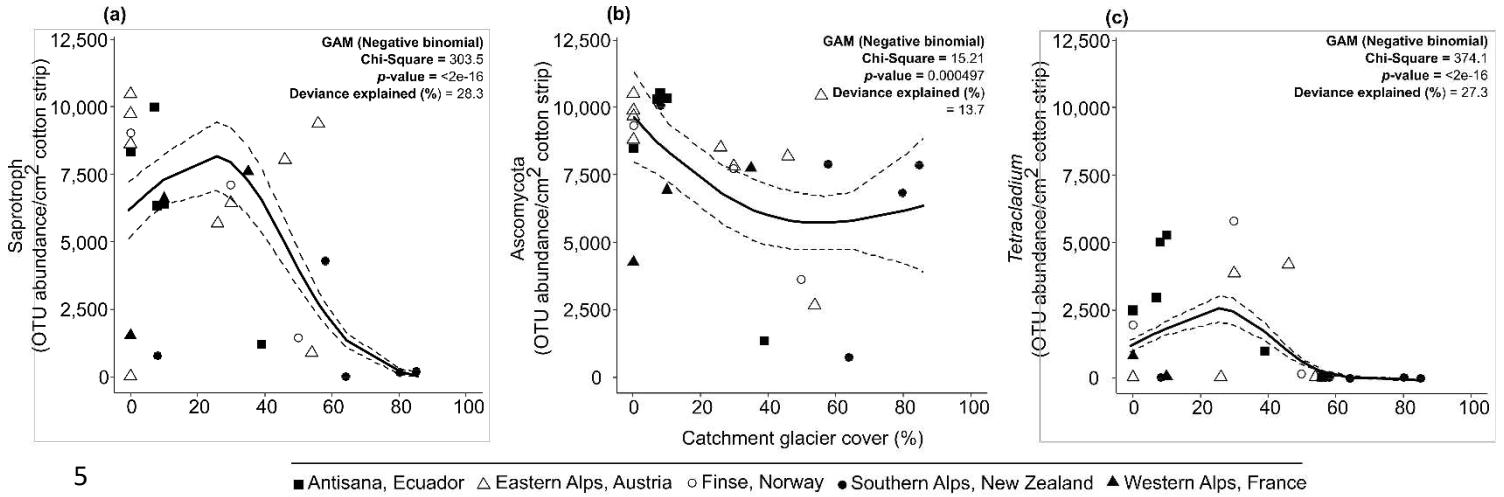
eprints@whiterose.ac.uk
<https://eprints.whiterose.ac.uk/>

1 **Supplementary information**

2

3 **Figures**

4



5

6 **Supplementary Figure 1: Fungal responses to changing catchment glacier cover.** The response

7 of subgroups of the fungal community (a - c) identified on cotton-strip assays incubated in glacierised

8 mountain rivers along a gradient of catchment glacier cover. For river sites in the Alaska Boundary

9 Range no amplification was detected. Solid lines are GAMs and dashed lines represent 95%

10 confidence intervals.

11

12

13

14

15

16

17

18

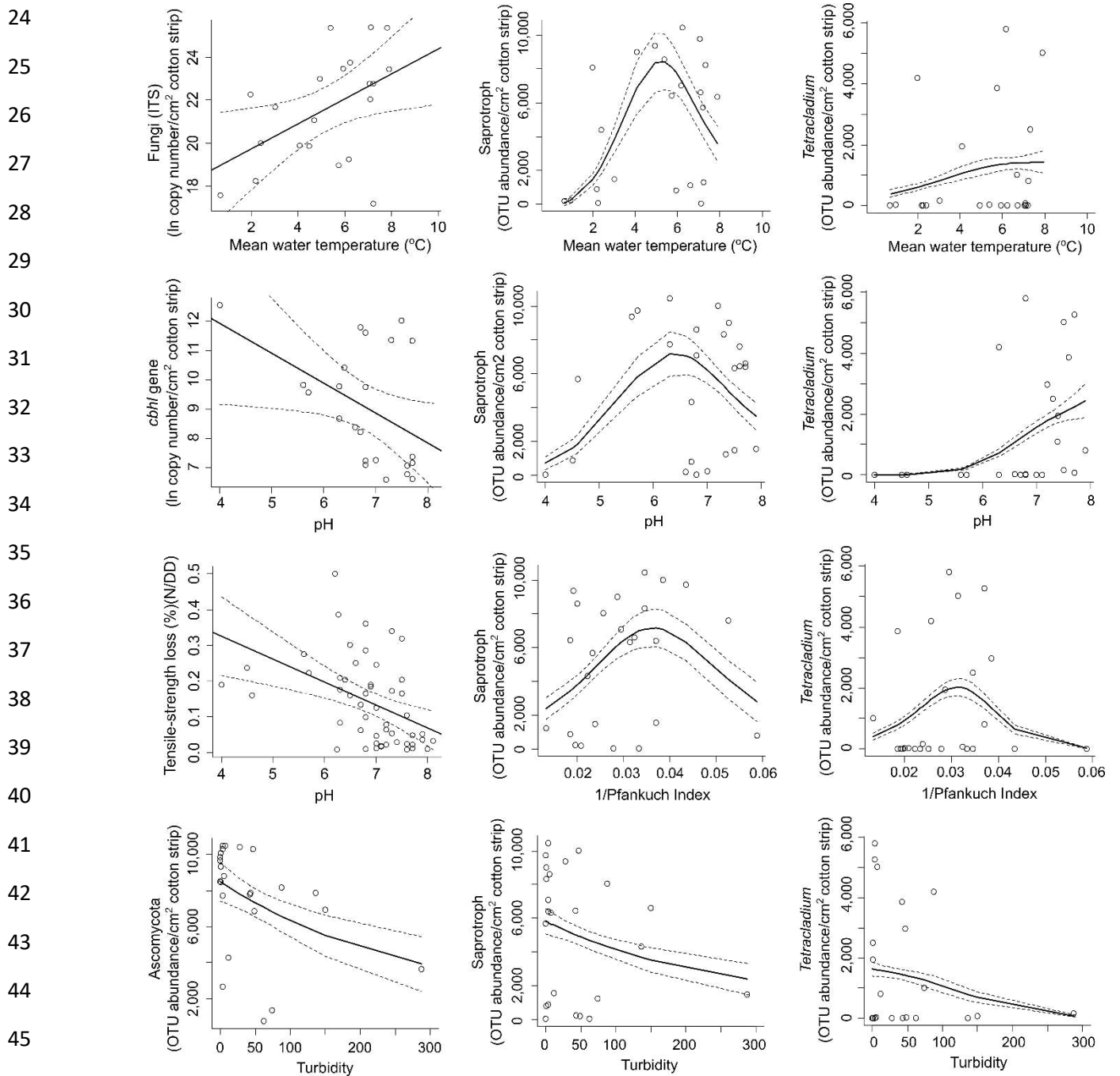
19

20

21

22

23



24
25
26
27
28
29
30
31
32
33
34
35
36
37
38
39
40
41
42
43
44
45
46

Supplementary Figure 2: Significant GLM/GAM relationships between physicochemical
parameters, nutrient concentrations (mg/L) and cotton-strip assay descriptors across six
glacierised mountain regions. The fungal community (ITS) is represented as a whole (ln qPCR
copy number/cm² cotton strip), and as subgroups (Ascomycota, *Tetracladium*, saprotrophs) (OTU
abundance/cm² cotton strip). The Pfankuch Index is a method for estimating the geomorphic channel
stability of rivers¹. Here, stability of the channel bottom is assessed, and higher scores represent
greater stability. Tensile-strength loss (%) (N/DD) pertains to the cotton-strip assay deployed at each

54 river site. Solid lines are GLMs or GAMs and dashed lines represent 95% confidence intervals.

55 Summary statistics are shown in Supplementary Table 2.

56

57

58

59

60

61

62

63

64

65

66

67

68

69

70

71

72

73

74

75

76

77

78

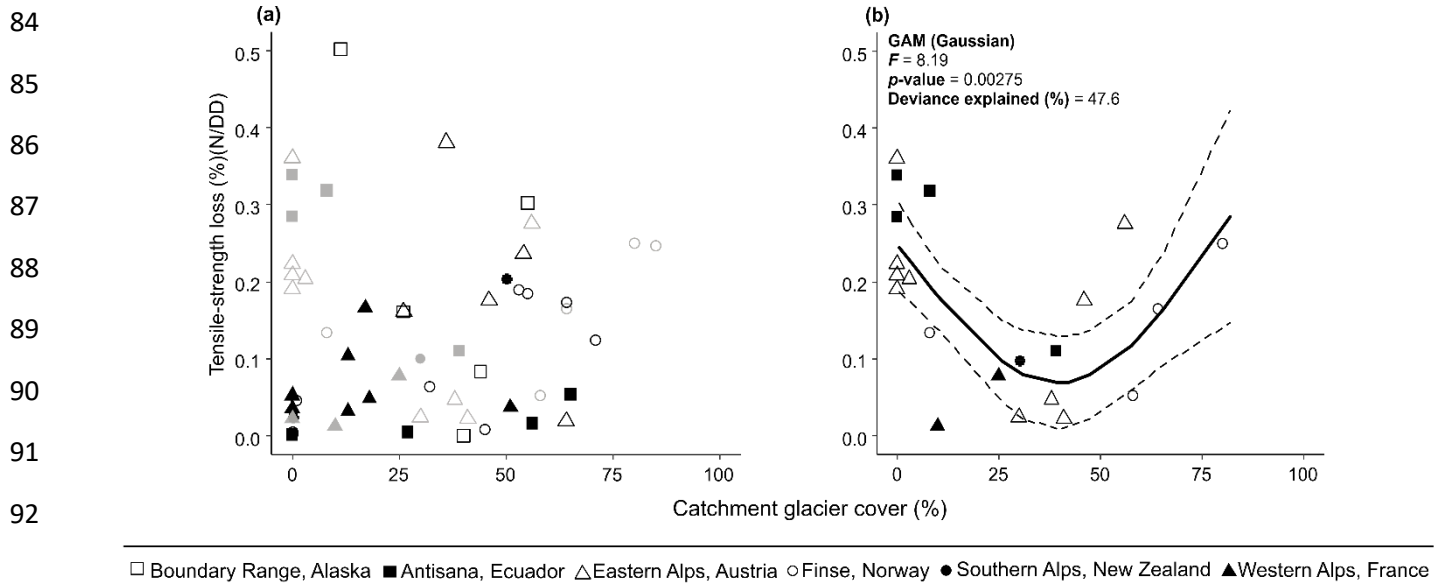
79

80

81

82

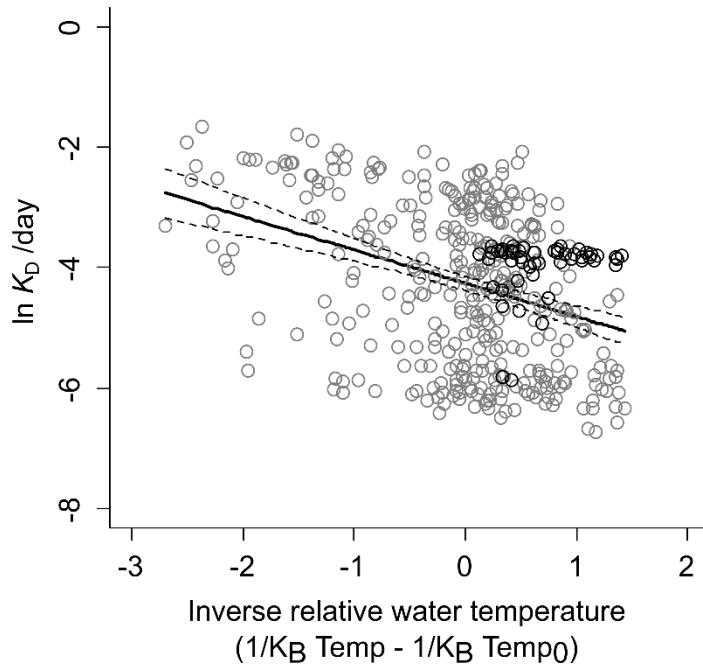
83



93 **Supplementary Figure 3: Tensile-strength loss values for glacierised mountain rivers spanning**
 94 **a gradient of catchment glacier cover.** (a) Mean tensile-strength loss per degree-day and
 95 catchment glacier cover of river sites. There was no relationship between tensile-strength loss and
 96 catchment glacier cover for all river sites (GAM(Gaussian), $F = 0.92$, $p = 0.404$, deviance explained
 97 (%) = 3.5) or those with no fungal ITS/*cbhl* amplification (black symbols: GAM(Gaussian), $F = 0.78$, p
 98 = 0.469, deviance explained (%) = 6.37). Samples with fungal ITS and/or *cbhl* amplification (grey
 99 symbols) showed a stronger relationship at $p < 0.10$ (GAM(Gaussian), $F = 3.12$, $p = 0.0624$, deviance
 100 explained (%) = 20.6). In contrast, (b) mean tensile-strength loss per degree-day and catchment
 101 glacier cover for only those river sites hosting *cbhl* amplification was significant at $p < 0.05$ (n.b. some
 102 but not all of these river sites showed fungal ITS amplification: see Supplementary Table 1).

103
104
105
106
107
108
109
110
111
112

113
114
115
116
117
118
119
120
121
122
123
124
125
126
127
128
129
130
131
132
133
134
135
136
137
138
139
140
141
142



Supplementary Figure 4: Temperature sensitivity of daily cellulose-decomposition rates for rivers in multiple biomes. An Arrhenius plot displaying the relationship between inverse relative river water temperature and non-temperature-adjusted (K_D) daily cellulose-decomposition rates (mean tensile-strength loss per river) for glacierised mountain rivers (\circ). Equivalent values are also displayed for rivers draining different biomes (\circ), as recorded by Tiegs et al. (2019)², showing that mountain river assays were representative of the global relationship. There was no significant relationship between water temperature and tensile-strength loss for sampled mountain rivers but the overall relationship across all data was significant (GLM: $F = 59.76$, $p = 8.52e-14$, deviance explained = 12.8%) (all circles, black lines). A combined analysis incorporated a random effect of the two data sources. Addition of mountain river data marginally increased the regression slope estimate (-0.55) compared to Tiegs et al. (2019)² (-0.68) but with clear overlap shown by the confidence intervals. K_B = Boltzmann constant (0.0000862), Temp = mean river site water temperature (K), Temp₀ = 283.15 K. Temperatures were normalised to 10 °C². Dashed lines represent 95% confidence intervals.

143 **Tables**144 **Supplementary Table 1: Study site information.** CGC(%) represents the percentage catchment

145 glacier cover of each river site. P = presence and A = absence of qPCR or PCR amplification of

146 fungal ITS and the fungal *cbhl* gene. Sites marked with * hosted fungal amplification (fungal ITS, *cbhl*

147 gene) and had upstream proglacial lakes.

148

Country	Region	Site code	Latitude (°)	Longitude (°)	CGC (%)	Fungal ITS	<i>cbhl</i> gene
Austria	Eastern Alps	A1	46.83104	11.04022	64	A	A
Austria	Eastern Alps	A2	46.83633	11.03612	41	P	P
Austria	Eastern Alps	A3	46.83981	11.03206	38	P	P
Austria	Eastern Alps	A4	46.84623	11.01827	30	P	P
Austria	Eastern Alps	A5	47.12213	12.63853	36	A	A
Austria	Eastern Alps	A6	47.12403	12.63864	3	P	P
Austria	Eastern Alps	A7	47.13204	12.63389	0	P	P
Austria	Eastern Alps	A8	47.13413	12.63749	26	P	A
Austria	Eastern Alps	A9	47.14075	12.65157	46	P	P
Austria	Eastern Alps	A10	47.13359	12.63351	0	P	P
Austria	Eastern Alps	A11	47.13269	12.63310	0	P	P
Austria	Eastern Alps	A12*	47.13403	12.63727	54	P	A
Austria	Eastern Alps	A13*	47.12971	12.28085	56	P	P
Austria	Eastern Alps	A14	47.13371	12.28345	0	P	P
Ecuador	Antisana	E1	-0.46987	-78.1829	0	A	A
Ecuador	Antisana	E2	-0.49556	-78.1961	27	A	A
Ecuador	Antisana	E3	-0.50470	-78.2162	0	A	P
Ecuador	Antisana	E4	-0.51282	-78.2158	0	A	P
Ecuador	Antisana	E5	-0.51374	-78.2174	8	P	P
Ecuador	Antisana	E6	-0.47128	-81.5010	65	A	A
Ecuador	Antisana	E7	-0.45508	-81.4760	56	A	A
Ecuador	Antisana	E8	-0.46530	-78.1652	39	A	P
Ecuador	Antisana	E9	-0.50550	-78.2162	7	A	A
Ecuador	Antisana	E10	-0.51306	-78.2156	10	P	P
France	Western Alps	F1	45.296718	6.645947	51	A	A
France	Western Alps	F2	45.297519	6.650509	0	A	A
France	Western Alps	F3	45.287004	6.669283	18	A	A
France	Western Alps	F4	45.296980	6.672500	0	P	A
France	Western Alps	F5	45.305088	6.669824	10	P	P
France	Western Alps	F6	45.312892	6.681206	13	A	A
France	Western Alps	F7	45.328562	6.625382	25	A	P
France	Western Alps	F8	45.346282	6.620300	17	A	A
France	Western Alps	F9	45.346917	6.616693	0	A	A
France	Western Alps	F10	45.361999	6.585158	13	A	A
France	Western Alps	F11	45.329039	6.625382	35	P	P
New Zealand	Southern Alps	NZ1	-43.47817	170.00835	50	P	A
New Zealand	Southern Alps	NZ2	-44.47523	168.72809	0	P	A
New Zealand	Southern Alps	NZ3	-44.50284	168.72032	30	P	P
Norway	Finse	N1	60.58883	7.44862	32	A	A
Norway	Finse	N2	60.58931	7.44816	45	A	A

Norway	Finse	N3	60.57460	7.47961	85	P	A
Norway	Finse	N4	60.57524	7.48529	71	A	A
Norway	Finse	N5	60.57416	7.49403	1	A	A
Norway	Finse	N6	60.56731	7.49382	8	P	P
Norway	Finse	N7	60.56763	7.50173	80	A	P
Norway	Finse	N8	60.57802	7.50746	58	P	P
Norway	Finse	N9	60.58072	7.51330	64	A	P
Norway	Finse	N10	60.58464	7.51981	55	A	A
Norway	Finse	N11	60.58464	7.51981	53	A	A
Norway	Finse	N12	60.58880	7.44874	0	A	A
Norway	Finse	N13	60.59002	7.55209	0	A	A
Norway	Finse	N14	60.59410	7.53861	64	A	A
USA	Alaska Boundary Range	USA1	58.364416	-134.478486	26	A	A
USA	Alaska Boundary Range	USA2	58.528439	-134.805948	40	A	A
USA	Alaska Boundary Range	USA3	58.404140	-134.581596	55	A	A
USA	Alaska Boundary Range	USA4	58.652052	-134.914173	11	A	A
USA	Alaska Boundary Range	USA5	58.528330	-134.805990	44	A	A

149

150

151

152

153

154

155

156

157

158

159

160

161

162

163

164

165

166

167

168

169 **Supplementary Table 2: GLM/GAM summary statistics.** Values relate to relationships displayed in
 170 Supplementary Figure 2. Water temperature = mean river water temperature (°C), Channel stability =
 171 1/Pfankuch Index, Turbidity = optical turbidity (NTU), *cbhl* = *cbhl* gene ln copy number/cm² cotton
 172 strip, ITS = fungal (ITS) ln copy number/cm² cotton strip, asco = Ascomycota OTU abundance, sapro
 173 = abundance of OTUs classified as hosting a saprotrophic trophic mode, *tetra* = *Tetracladium* OTU
 174 abundance and TS loss = tensile-strength loss (%) (N/DD).

175

176

Variables	Model (Distribution)	χ^2 / F	p-value	Deviance explained (%)
Water temperature				
<i>cbhl</i>	GLM (Gaussian)	4.02	0.0593	17.5
ITS	GLM (Gaussian)	6.00	0.0241	24.0
asco	GLM (Gaussian)	2.35	0.14075	10.5
sapro	GAM (Negative binomial)	173.4	< 2e-16	19.5
<i>tetra</i>	GAM (Negative binomial)	53.3	2.66e-12	2.48
pH				
<i>cbhl</i>	GLM (Gaussian)	4.59	0.0441	17.9
ITS	GAM (Gaussian)	1.243	0.313	12.8
asco	GLM (Gaussian)	0.2082	0.6524	0.9
sapro	GAM (Negative binomial)	73.9	< 2e-16	6.97
<i>tetra</i>	GAM (Negative binomial)	486.7	< 2e-16	25.2
TS loss	GLM (Gaussian)	11.57	< 0.0029	18.2
Channel stability				
<i>cbhl</i>	GAM (Gaussian)	1.30	0.302	14.8
ITS	GAM (Gaussian)	0.42	0.663	4.72
asco	GLM (Gaussian)	4.15	0.05322	15.3
sapro	GAM (Negative binomial)	39.33	2.88e-09	5.98
<i>tetra</i>	GAM (Negative binomial)	210.0	< 2e-16	9.36
TS loss	GLM (Gaussian)	1.46	0.2327	3.0
Turbidity				
<i>cbhl</i>	GAM (Gaussian)	4.91	0.0181	32.9
ITS	GLM (Gaussian)	1.66	0.212	7.3
asco	GAM (Negative binomial)	11.94	0.00256	10.3
sapro	GAM (Negative binomial)	18.15	0.00114	2.9
<i>tetra</i>	GAM (Negative binomial)	263.9	< 2e-16	9.6
TS loss	GLM (Gaussian)	0.005	0.946	8.8

177

178 **Supplementary Table 3: Fungal responses to reducing catchment glacier cover and tensile-**
 179 **strength loss.** Wald statistics illustrating fungal (ITS) OTUs whose relative abundance was
 180 associated significantly ($Pr(>wald) = < 0.05$) with either catchment glacier cover (%CGC) or tensile-
 181 strength loss (TS loss). Values were calculated with *manyglm* analysis using the *mvabund* package of
 182 R³. The +/- signs indicate if relative OTU abundance increased or decreased with reductions in
 183 catchment glacier cover and tensile-strength loss across the six glacierised mountain regions.

184

185	OTU Identification	Wald	Pr(>wald)	%CGC	TS
186		value			loss
187	<i>Fungi (ITS)</i>				
187	<i>Lemonniera centrosphaera</i>	110.28	0.002	+	
188	<i>Tetracladium</i> sp.	38.22	0.010	+	
189	Unclassified	30.84	0.031	-	
189	Unclassified	40.89	0.003	-	
190	Unclassified	45.21	0.002	-	
191	Helotiales sp.	50.27	0.002	+	
192	Unclassified	50.25	0.002	-	
192	Unclassified	29.70	0.045	-	
193	Unidentified	36.95	0.013	-	
194	<i>Tetracladium marchalianum</i>	61.52	0.002	+	
195	Unclassified	90.67	0.002	-	
195	Unclassified	31.57	0.025	-	
196	Leotiomycetes sp.	116.81	0.002	-	
197	Unclassified	31.81	0.024	-	
198	<i>Tetracladium</i> sp.	37.97	0.011	+	
198	Ascomycota sp.	74.88	0.002	-	
199	<i>Tetracladium</i> sp.	32.36	0.023	+	
200	Ascomycota sp.	54.43	0.002	+	
201	<i>Tetracladium psychrophilum</i>	94.84	0.045		-

202

203

204

205

206

207

208 **Supplementary Table 4: Latitudinal position was not associated with changes in aquatic**
 209 **cellulose-decomposition rates.** GLMM and GAMM summary statistics for fixed effect models
 210 (Figure 1 and Supplementary Figure 1). %CGC = catchment glacier cover (%), TS loss = tensile-
 211 strength loss (%) (N/DD), ITS = fungal (ITS) In copy number/cm² cotton strip, *cbhl* = *cbhl* gene In copy
 212 number/cm² cotton strip, asco = Ascomycota OTU abundance, *tetra* = *Tetracladium* OTU abundance,
 213 sapro = saprotroph OTU abundance. Addition of absolute latitude did not improve model performance
 214 (higher AIC values) for all measured relationships.

215

	Value	SE	<i>t</i>	<i>p</i> -value	<i>F</i> ² /Deviance explained (%)	AIC
GLMM						
ITS vs %CGC	-0.05	0.02	-2.83	0.0101	0.24	105.22
TS loss vs ITS	0.02	0.01	2.56	0.0193	0.22	-35.93
TS loss vs <i>cbhl</i>	0.04	0.01	4.73	< 0.000147	0.52	-44.73
GAMM						
asco vs %CGC	-48.66	19.52	-2.49	0.0203	21.3	468.35
<i>tetra</i> vs %CGC	-16.99	14.38	-1.81	0.24946	5.7	454.07
sapro vs %CGC	-67.12	24.80	-2.71	0.0126	24.2	480.32
<i>cbhl</i> vs %CGC	-0.05	0.01	-3.45	0.00243	36.1	92.00

225

226

227

228

229

230

231

232

233 **Supplementary references**

- 234 1. Pfankuch, D. J. *Stream Reach Inventory and Channel Stability Evaluation* (Northern Region,
235 Montana, US Department Forest Service, 1975).
- 236 2. Tiegs, S. D. et al.. Global patterns and drivers of ecosystem functioning in rivers and riparian
237 zones. *Science Advances* **5**, (2019).
- 238 3. Wang, Y., Maumann, U., Wright, S. & Warton, D. *Mvabund: Statistical methods for analysing*
239 *multivariate abundance data*. [Online]. [Accessed 2 November 2018]. Available from: [https://cran.r-](https://cran.r-project.org/package=mvabund)
240 [project.org/package=mvabund](https://cran.r-project.org/package=mvabund) (2018).